Sensors and Materials, Vol. 35, No. 2 (2023) 483–489
MYU Tokyo

S & M 3185

Development of In-doped RbBr Transparent Ceramics with Optically Stimulated Luminescence Properties

Takumi Kato,[1*] Hiromi Kimura,[2] Kai Okazaki,[1]
Daisuke Nakauchi,[1] Noriaki Kawaguchi,[1] and Takayuki Yanagida[1]

[1]Nara Institute of Science and Technology (NAIST), 8916-5, Takayama-cho, Ikoma-shi, Nara 630-0192, Japan
[2]National Institute of Advanced Industrial Science and Technology (AIST), 1-1-1, Tsukuba, Ibaraki 305-8569, Japan

(Received September 30, 2022; accepted January 10, 2023)

Keywords: RbBr, indium, transparent ceramic, OSL, dosimeter

As new alternative optically stimulated luminescence (OSL) materials to Eu-doped CsBr and Tl-doped RbBr, we synthesized In-doped RbBr transparent ceramics by spark plasma sintering. All the ceramics had a transmittance of approximately 60% from 300 to 800 nm. In its photoluminescence (PL) and scintillation spectra, In-doped RbBr showed an emission peak at 500 nm due to $^3P_1 \rightarrow ^1S_0$ transitions of In^+ ions. The PL and scintillation decay time constants were approximately 4.1 μs. OSL was observed upon optical stimulation at 700 nm. The 0.5% In-doped RbBr had a linear OSL response in the dose range from 0.3 mGy to 3 Gy.

1. Introduction

Storage phosphors have the function of temporarily storing incident radiation energy in the form of electrons and holes. The stored energy can be read out by external stimulation to emit light. When the external stimulation is heat or light, the resultant emissions are called thermally stimulated luminescence (TSL) and optically stimulated luminescence (OSL), respectively. Since the intensity of the resultant emissions is proportional to the irradiated dose, such phosphors have been used in imaging plates (IPs)[1,2] and personal and environmental dose-monitoring devices.[3,4] When storage phosphors are used for IPs, the desired properties are high luminescence output, wide dynamic range, short decay time (~10 μs), low fading, and effective X-ray absorption. In the case of personal dose-monitoring devices, the effective atomic number (Z_{eff}) of the storage phosphors should be close to that of the human body (Z_{eff} = 7.29), based on the composition of $C_5H_{40}O_{18}N$, from the viewpoint of bioequivalence.[5]

Conventionally, storage phosphors such as Eu-doped CsBr and Tl-doped RbBr have been developed and used for commercial IPs.[6,7] Eu-doped CsBr and Tl-doped RbBr crystals show high OSL intensities at around 440 and 400 nm, respectively, making them suitable for use in a photomultiplier tube (PMT).[8,9] In addition, these phosphors can be stimulated by a conventional He-Ne laser or semiconductor laser. The photoluminescence (PL), OSL, and TSL properties of RbBr doped with Eu, Tb, Sm, and Yb have also been reported.[10–13] Moreover, powder and thin-

*Corresponding author: e-mail: kato.takumi.ki5@ms.naist.jp
https://doi.org/10.18494/SAM4137

ISSN 0914-4935 © MYU K.K.
https://myukk.org/

film phosphors have been used for conventional IPs, but transparent ceramics have recently been reported to be useful as storage phosphors because of their transparency.(14,15)

The aim of this study is to develop In-doped RbBr transparent ceramics with different concentrations of In and evaluate the effects of In doping on their optical, scintillation, and OSL properties. Indium generally takes various valence states such as +1 and +3. For example, indium oxide contains indium in the +3 state, and In^{3+} ions cannot contribute to luminescence. On the other hand, In^{+} is used as an ns^2-type luminescence center in several phosphors. The ns^2-type ions (n = 4, 5, 6) can emit photons because of their ns^2 electron configuration in the ground state and their ns^1np^1 configuration in the excited state. The emission properties of several ns^2-type ions have been reported, including alkali halides and oxides.(16–20) Because Tl^{+} is also categorized as an ns^2-type ion, In^{+} ions can be an alternative dopant owing to their similar electron configuration and ionic radius to Tl^{+}. However, the luminescence properties of In-doped RbBr such as its PL, scintillation, and OSL have not yet been investigated.

2. Materials and Methods

In-doped RbBr samples were prepared in the same way as in our previous report.(21) RbBr (> 99%, Mitsuwa Chemical) and InBr (99.99%, Kojundo Chemical) were used as raw powders. After sintering, the wide surfaces of the obtained samples were mechanically polished using various sandpapers (600–3000 grits).

Regarding the basic optical properties, the in-line transmittance spectrum was measured using a spectrometer (SolidSpec-3700, Shimadzu) in the range of 200 to 800 nm with 1 nm intervals. Additionally, the PL excitation/emission contour plot and quantum yield (*QY*) were obtained using a Quantaurus-QY system (C11347, Hamamatsu Photonics). To estimate the decay time constants, the PL decay curves were evaluated using a Quantaurus-τ system (C11367, Hamamatsu Photonics). Scintillation spectra were measured with our original setup.(22) An X-ray-excited fluorescence lifetime photometer (Hamamatsu Photonics) was used to measure scintillation decay curves.(23) To evaluate OSL dose response functions, we measured OSL spectra and curves using a spectrofluorometer (FP-8600, JASCO). In these measurements, an X-ray generator (XRB80N100/CB, Spellman) was used as a radiation source, which was equipped with an X-ray tube with a W anode target. This voltage had been fully rectified, and the average X-ray energy was 26 keV. The irradiated dose was calibrated using an air-filled ionization chamber (TN30013, PTW).

3. Results and Discussion

Transparent In-doped RbBr ceramics were obtained, as illustrated in Fig. 1. The sample thickness was about 0.90 mm. All the samples were transparent, regardless of the In concentration. Under UV light (254 nm), all the samples exhibited sky-blue luminescence. To confirm the transparency of the ceramic samples, diffuse transmittance spectra were recorded, as shown in Fig. 2. All the samples had a transmittance of approximately 60% from 300 to 800 nm, and several absorption bands were observed between 200 and 300 nm, which were ascribed to $^1S_0 \rightarrow {}^1P_1$, $^1S_0 \rightarrow {}^3P_2$, and $^1S_0 \rightarrow {}^3P_1$ transitions.(24–26)

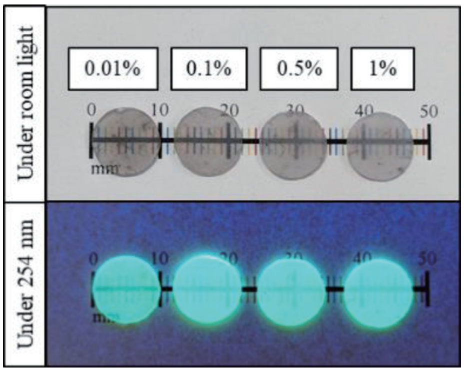

Fig. 1. (Color online) Appearance of the In-doped RbBr transparent ceramics.

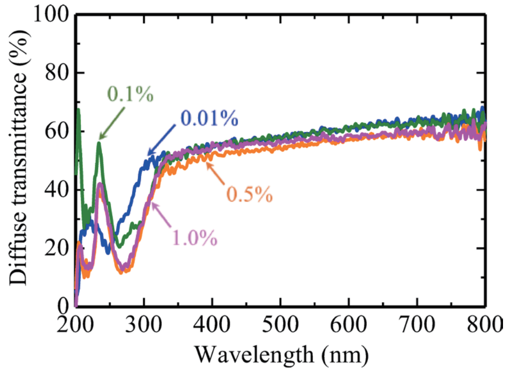

Fig. 2. (Color online) Diffuse transmittance spectra of all the samples.

Figure 3 shows a PL contour map of the 0.1% In-doped RbBr. Here, because the PL excitation and emission spectra of all the samples had similar shapes, the PL contour map of the 0.1% In-doped RbBr is shown as a representative. An emission band was detected at 500 nm under excitations of ~250 and 300 nm. The excitation wavelengths roughly coincided with the absorption wavelengths observed in the diffuse transmittance spectrum. The emission at 500 nm is attributed to $^3P_1 \rightarrow {}^1S_0$ transitions of In^+ ions.(25,26) The PL *QY* of each sample became maximum when the excitation was 300 nm, and the *QY* values of the 0.01, 0.1, 0.5, and 1.0% In-doped RbBr were calculated to be 3.3, 33.4, 7.4, and 7.1%, respectively. A decrease in PL *QY* is associated with concentration quenching, which is often observed in common phosphors.(27–30) Compared with those of Eu-doped CsBr transparent ceramics,(31) the *QY* values were up to 10 times higher. Figure 4 shows PL decay curves of all the samples. The excitation and monitored wavelengths were 280 and 500 nm, respectively. The PL decay curves were well reproduced by an exponential decay function, and the derived decay time constant was ~4.1 μs. Compared with the values in prior studies,(24,32) the value is reasonable for $^3P_1 \rightarrow {}^1S_0$ transitions of In^+ ions.

Figure 5 displays X-ray-induced scintillation spectra of all the samples. For all the samples, a scintillation peak was detected at 500 nm, as with the PL spectra. The peak intensity of the 0.5% In-doped RbBr was the highest among the samples. X-ray-induced scintillation decay curves of all the samples are shown in Fig. 6. The measured scintillation decay curves were approximated by an exponential decay function. The obtained value was ~4.1 μs, which was the same as the PL decay time constant.

Figure 7 shows an OSL curve of the 0.5% In-doped RbBr measured during constant stimulation at 700 nm. The inset shows OSL stimulation and emission spectra of all the samples. The samples were irradiated with 1 Gy of X-rays before measurements. A stimulation peak was observed at 700 nm, and the OSL emission peak at 450 nm was dominant under the 700 nm stimulation. The emission intensity decreased with continuous stimulation; therefore, the emission peak observed under the 700 nm stimulation is entirely due to the OSL phenomena. Although the wavelength of that OSL was shorter than those of PL and scintillation, the OSL peak may be due to $^3P_1 \rightarrow {}^1S_0$ transitions of In^+ ions. In this measurement, the OSL signals were gradually read out from a shorter wavelength using a diffraction grating, and signal fading

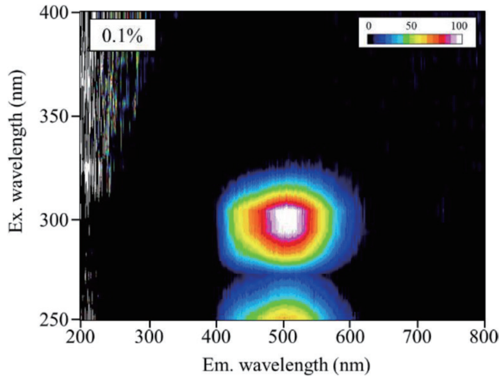

Fig. 3. (Color online) PL contour map of the 0.1% In-doped RbBr.

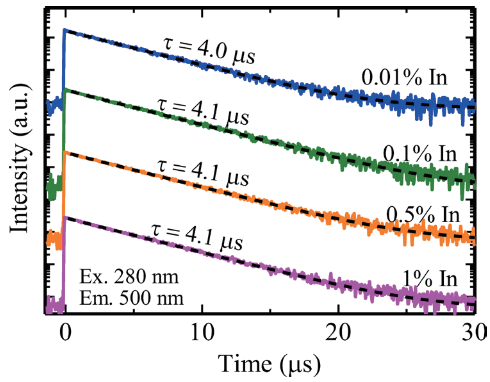

Fig. 4. (Color online) PL decay curves of all the samples.

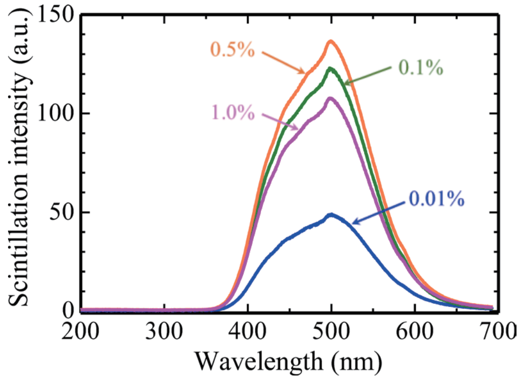

Fig. 5. (Color online) X-ray-induced scintillation spectra of all the samples.

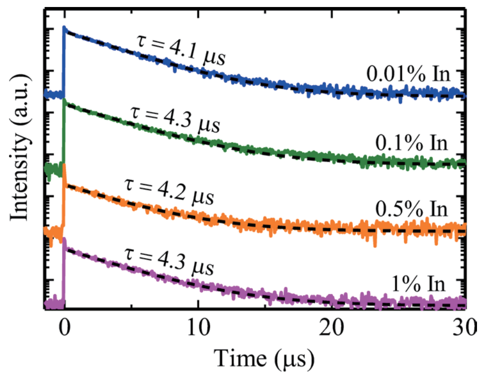

Fig. 6. (Color online) X-ray-induced scintillation decay curves of all the samples.

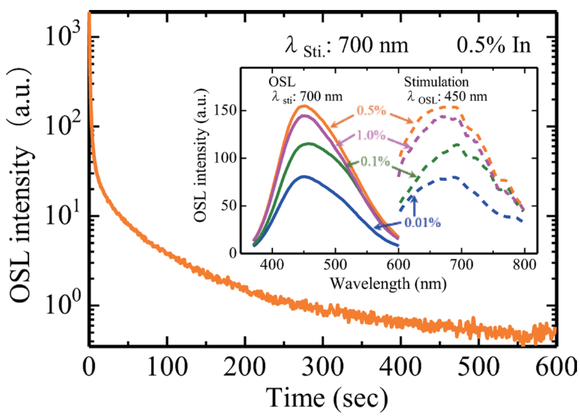

Fig. 7. (Color online) OSL curve of the 0.5% In-doped RbBr. The inset shows OSL stimulation and emission spectra of all the samples.

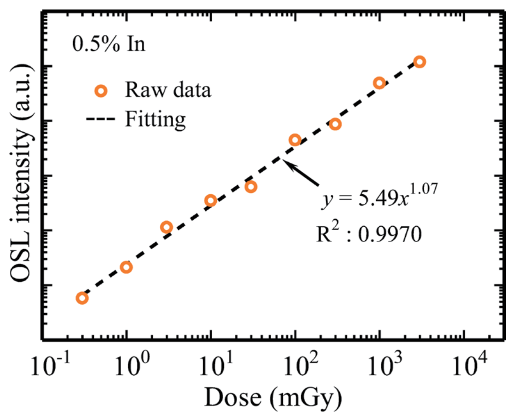

Fig. 8. (Color online) OSL dose response function of the 0.5% In-doped RbBr.

occurred during measurement. As a result, an OSL wavelength shorter than those of PL and scintillation was observed. In contrast, the stimulation peak at around 700 nm was due to F centers.(7) The OSL intensity was highest when the In concentration was 0.5%, whereas the PL *QY* was maximum in the 0.1% In-doped RbBr. Generally, the OSL intensity is proportional to the probability that secondary electrons are transported up to trapping centers, the probability that electrons released from trapping centers are transported to luminescence centers, and the recombination efficiency of luminescence centers.(33) Hence, if the number of F centers was not changed by In doping, it could be interpreted that the probability that electrons released from F centers are transported to In was increased by the high In concentration.

Figure 8 shows the OSL dose response function of the 0.5% In-doped RbBr. The vertical axis represents the integrated intensity of each OSL emission spectrum from 370 to 600 nm. Although the irradiation dose was tested from 0.01 mGy to 10 Gy, the OSL signal was detected in the dose range between 0.3 mGy and 3 Gy. For the irradiation dose of 10 Gy, we could not measure the correct OSL intensity because it exceeded the upper detection limit of the equipment. The linearity was confirmed from the coefficient of determination (R^2) of 0.9970 derived from the least-squares fitting of the experimental data with a power function ($y = ax^b$). As a result, the detection limit of 0.3 mGy was worse than that of Eu-doped CsBr (0.01 mGy) reported in a previous study.(34)

4. Conclusions

In-doped RbBr transparent ceramics were synthesized by spark plasma sintering. The PL spectra of In-doped RbBr showed a PL emission peak at around 500 nm, originating from $^3P_1 \rightarrow {}^1S_0$ transitions of In^+ ions. Under also X-ray irradiation, In-doped RbBr showed scintillation peaks at around 500 nm. The decay time constant of the luminescence was within 10 μs, indicating that In-doped RbBr can be applied to IPs. After X-ray irradiation, In-doped RbBr showed OSL upon optical stimulation at 700 nm. In the OSL process, the luminescence and trapping centers are In^+ ions and F centers, respectively. Using In-doped RbBr, it is possible to measure radiation doses from 0.3 mGy to 3 Gy with good linear response.

Acknowledgments

This work was supported by Grants-in-Aid for Scientific A (22H00309), Scientific B (22H02939, 21H03733, and 21H03736), and Exploratory Research (22K18997) from Japan Society for the Promotion of Science. The Cooperative Research Project of Research Center for Biomedical Engineering, TEPCO Memorial Foundation, Nakatani Foundation, and KRF Foundation are also acknowledged.

References

1 H. Nanto, A. Nishimura, M. Kuroda, Y. Takei, Y. Nakano, T. Shoji, T. Yanagita, and S. Kasai: Nucl. Instrum. Methods Phys. Res. Sect. A **580** (2007) 278. https://doi.org/10.1016/j.nima.2007.05.155
2 H. Nanto, G. Okada, K. Hirasawa, Y. Koguchi, W. Shinozaki, S. Ueno, Y. Yanagida, F. d'Errico, and T. Yamamoto: Sens. Mater. **34** (2022) 757. https://doi.org/10.18494/SAM3686
3 S. W. S. McKeever: Radiat. Meas. **46** (2011) 1336. https://doi.org/10.1016/j.radmeas.2011.02.016
4 P. Leblans, D. Vandenbroucke, and P. Willems: Materials **4** (2011) 1034. https://doi.org/10.3390/ma4061034
5 C. A. Jayachandran: Phys. Med. Biol. **16** (1971) 617. https://doi.org/10.1088/0031-9155/16/4/005
6 P. Hackenschmied, G. Zeitler, M. Batentschuk, A. Winnacker, B. Schmitt, M. Fuchs, E. Hell, and W. Knüpfer: Nucl. Instrum. Methods Phys. Res. Sect. B **191** (2002) 163. https://doi.org/10.1016/S0168-583X(02)00544-X
7 H. Von Seggern, A. Meijerink, T. Voigt, and A. Winnacker: J. Appl. Phys. **66** (1989) 4418. https://doi.org/10.1063/1.343936
8 H. von Seggern: Brazilian J. Phys. **29** (1999) 254. https://doi.org/10.1590/S0103-97331999000200008
9 H. Nanto: Sens. Mater. **30** (2018) 327. https://doi.org/10.18494/SAM.2018.1803
10 S. Schweizer, U. Rogulis, S. Assmann, and J. M. Spaeth: Radiat. Meas. **33** (2001) 483. https://doi.org/10.1016/S1350-4487(01)00035-X
11 P. K. Manimozhi, G. Muralidharan, S. Selvasekarapandian, and J. Malathi: Phys. Status Solidi Basic Res. **244** (2007) 726. https://doi.org/10.1002/pssb.200642286
12 P. K. Manimozhi and G. Muralidharan: Nucl. Instrum. Methods Phys. Res. Sect. B **267** (2009) 807. https://doi.org/10.1016/j.nimb.2008.12.022
13 I. M. Mejeha: Glob. J. Pure Appl. Sci. **13** (2007) 591. https://doi.org/10.4314/gjpas.v13i4.16762
14 J. Xu, J. Ueda, K. Kuroishi, and S. Tanabe: Scr. Mater. **102** (2015) 47. https://doi.org/10.1016/j.scriptamat.2015.01.029
15 T. Kato, D. Nakauchi, N. Kawaguchi, and T. Yanagida: Curr. Appl. Phys. **20** (2020) 1195. https://doi.org/10.1016/j.cap.2020.08.011
16 K. Polák and E. Mihóková: Opt. Mater. **32** (2010) 1280. https://doi.org/10.1016/j.optmat.2010.05.006
17 T. Kawai and A. Iguchi: J. Lumin. **207** (2019) 58. https://doi.org/10.1016/j.jlumin.2018.11.008
18 D. Onoda, H. Kimura, T. Kato, D. Nakauchi, N. Kawaguchi, and T. Yanagida: Jpn. J. Appl. Phys. **60** (2021) 1. https://doi.org/10.35848/1347-4065/ac384b
19 T. Kato, D. Nakauchi, N. Kawaguchi, and T. Yanagida: Sens. Mater. **32** (2020) 1411. https://doi.org/10.18494/SAM.2020.2742
20 H. Fukushima, D. Shiratori, D. Nakauchi, T. Kato, N. Kawaguchi, and T. Yanagida: Sens. Mater. **34** (2022) 717. https://doi.org/10.18494/SAM3691
21 H. Kimura, T. Kato, D. Nakauchi, N. Kawaguchi, and T. Yanagida: Nucl. Instrum. Methods Phys. Res. Sect. B **478** (2020) 137. https://doi.org/10.1016/j.nimb.2020.06.010
22 T. Yanagida, K. Kamada, Y. Fujimoto, H. Yagi, and T. Yanagitani: Opt. Mater. **35** (2013) 2480. https://doi.org/10.1016/j.optmat.2013.07.002
23 T. Yanagida, Y. Fujimoto, T. Ito, K. Uchiyama, and K. Mori: Appl. Phys. Express. **7** (2014) 5. https://doi.org/10.7567/APEX.7.062401
24 H. Masai, Y. Yamada, S. Okumura, T. Yanagida, Y. Fujimoto, Y. Kanemitsu, and T. Ina: Sci. Rep. **5** (2015) 1. https://doi.org/10.1038/srep13646
25 V. Nagirnyi, P. Vaino, and S. Zazubovich: Phys. Status Solidi. **167** (1991) 659. https://doi.org/10.1002/pssb.2221670227
26 V. S. Sivasankar, K. Schmitt, and P. W. M. Jacobs: J. Lumin. **33** (1985) 409. https://doi.org/10.1016/0022-2313(85)90110-3

27 T. Yanagida, Y. Fujimoto, H. Masai, G. Okada, T. Kato, D. Nakauchi, and N. Kawaguchi: Sens. Mater. **33** (2021) 2179. https://doi.org/10.18494/SAM.2021.3315
28 M. Akatsuka, N. Daisuke, K. Takumi, N. Kawaguchi, and T. Yanagida: Sens. Mater. **34** (2022) 619. https://doi.org/10.18494/SAM3692
29 Y. Takebuchi, T. Kato, D. Nakauchi, N. Kawaguchi, and T. Yanagida: Optik **260** (2022) 677. https://doi.org/10.1016/j.ijleo.2022.169079
30 R. Nakamori, N. Kawano, A. Takaku, D. Onoda, Y. Takebuchi, H. Fukushima, T. Kato, K. Shinozaki, and T. Yanagida: Sens. Mater. **34** (2022) 707. https://doi.org/10.18494/SAM3689
31 H. Kimura, T. Kato, M. Akatsuka, D. Nakauchi, G. Okada, N. Kawaguchi, and T. Yanagida: Radiat. Meas. **135** (2020) 106367. https://doi.org/10.1016/j.radmeas.2020.106367
32 D. Klick and H. G. Drickamer: Phys. Rev. B **17** (1978) 952. https://doi.org/10.1103/PhysRevB.17.952
33 S. W. S. McKeever: Nucl. Instruments Methods Phys. Res. B **184** (2001) 29. https://doi.org/10.1016/S0168-583X(01)00588-2
34 N. M. Winch and A. Edgar: Phys. Med. Imaging **8313** (2012) 83135E. https://doi.org/10.1117/12.911146